

# Observation of pseudogap behavior in a strongly interacting Fermi gas

J. P. Gaebler<sup>1</sup>, J. T. Stewart<sup>1</sup>, T. E. Drake<sup>1</sup> and D. S. Jin<sup>1</sup>, A. Perali<sup>2</sup>, P. Pieri<sup>2</sup> and G. C. Strinati<sup>2</sup>

<sup>1</sup> *JILA, National Institute of Standards and Technology (NIST) and University of Colorado,*

*Department of Physics, University of Colorado, Boulder, CO 80309, USA and*

<sup>2</sup> *Dipartimento di Fisica, Università di Camerino, I-62032 Camerino, Italy*

(Dated: August 27, 2018)

Ultracold atomic Fermi gases present an opportunity to study strongly interacting Fermi systems in a controlled and uncomplicated setting. The ability to tune attractive interactions has led to the discovery of superfluidity in these systems with an extremely high transition temperature [1, 2], near  $\frac{T}{T_F} = 0.2$ . This superfluidity is the electrically neutral analog of superconductivity; however, superfluidity in atomic Fermi gases occurs in the limit of strong interactions and defies a conventional BCS description. For these strong interactions, it is predicted that the onset of pairing and superfluidity can occur at different temperatures [3–5]. This gives rise to a pseudogap region where, for a range of temperatures, the system retains some of the characteristics of the superfluid phase, such as a BCS-like dispersion and a partially gapped density of states, but does not exhibit superfluidity. By making two independent measurements: the direct observation of pair condensation in momentum space and a measurement of the single-particle spectral function using an analog to photoemission spectroscopy [6], we directly probe the pseudogap phase. Our measurements reveal a BCS-like dispersion with back-bending near the Fermi wave vector  $k_F$  that persists well above the transition temperature for pair condensation.

In conventional superconductors, fermion pairs and superconductivity appear simultaneously at  $T_c$ . The single-particle, or fermionic, excitation spectrum of a conventional superconductor follows a BCS dispersion given by

$$E_s = \mu \pm \sqrt{(\epsilon_k - \mu)^2 + \Delta^2}, \quad (1)$$

where  $\epsilon_k = \hbar^2 k^2 / 2m$ ,  $\mu$  is the chemical potential, and  $\Delta$  is the superfluid order parameter. The lower branch of the dispersion (minus sign in Eqn. 1), which is the occupied one at low temperature, has a positive slope at low momentum and then turns around and has a negative slope at high momentum. This “back-bending” behavior arises because of the excitation gap and is a characteristic signature of superconductivity. In unconventional superconductors, such as high  $T_c$  superconductors, this back-bending in the dispersion has been observed both below [7] and, remarkably, above  $T_c$  [8]. The observation of back-bending above  $T_c$  represents a dramatic departure from conventional BCS theory, which predicts that the

normal state above  $T_c$  is a Fermi liquid with a monotonically increasing single-branch dispersion and a density of states that is smooth through the Fermi surface. The departure from a conventional BCS description above  $T_c$  in the form of a gapped excitation spectra is the essence of the pseudogap.

A satisfactory explanation of the origin and nature of the observed pseudogap phase in high  $T_c$  superconductors has remained elusive due to the complexity of the materials. In contrast, ultracold atomic gases are relatively free of complexity, for example, having no underlying lattice structure, impurities, or domain boundaries. Moreover, the interactions responsible for pairing and superfluidity in ultracold atom gases are well understood at the few-body level. As a result, these systems are ideally suited for investigating the prediction of a pseudogap phase due to pre-formed pairs. There is much scientific literature on the topic of the pseudogap in strongly interacting atom gases with wide-ranging viewpoints and conclusions [4, 9–18], including a recent article that predicts no pseudogap phase at all [19]. In some theories, the pseudogap phase is predicted to have a BCS-like dispersion (Eqn. 1), but where  $\Delta$  is no longer the superfluid order parameter but instead corresponds to an excitation gap due to the formation of incoherent pairs [4, 9–18]. However, for the atomic gases, there is not yet experimental data to establish the existence of a pseudogap phase and confirm its properties. Radio frequency (rf) spectroscopy experiments that probe excitations have been performed above and below the critical temperature [20, 21], but their interpretation relies on assuming a specific dispersion relation and therefore they cannot be used to distinguish between a pseudogap and a normal phase [14, 19].

The question is then, do we have the necessary measurement tools to look for pseudogap physics in the neutral atom gas system? To probe the defining properties of a pseudogap regime one needs both a measurement of the transition temperature as well as a probe of the single-particle excitation spectra. In the atomic gas system, the onset of the superfluid phase is clearly detected through the observation of momentum-space condensation of atom pairs [22]. To probe the single-particle excitation spectra, we use a technique recently developed for atoms that uses momentum-resolved rf spectroscopy to realize an analog of photoemission spectroscopy [6]. Using these two measurements: the direct observation

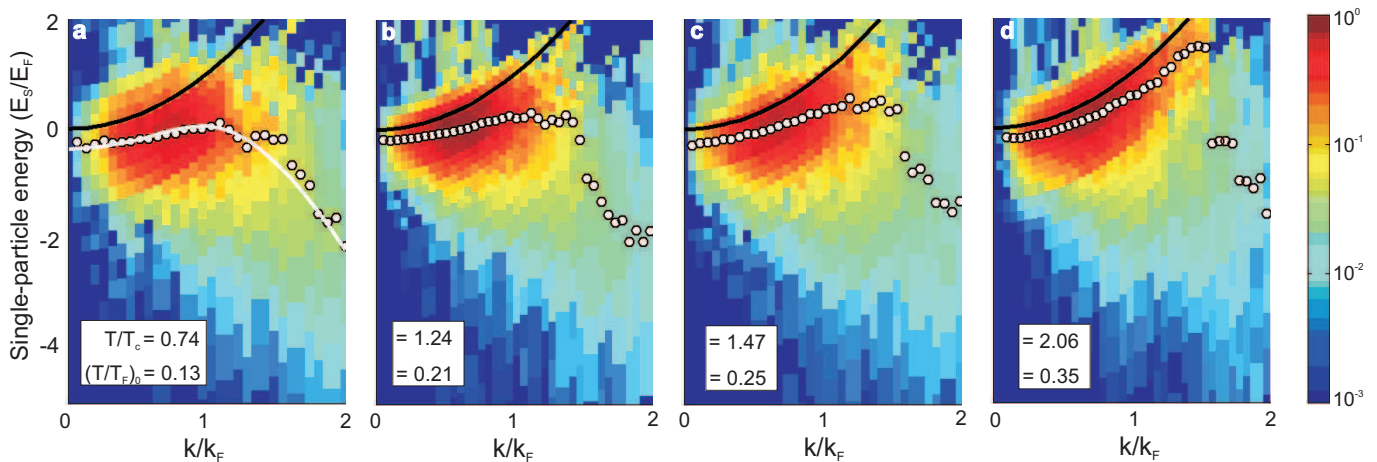


FIG. 1: **Photoemission spectra throughout the pseudogap regime.** Spectra are shown for Fermi gases at four different temperatures, each with an interaction strength characterized by  $(k_F a)^{-1} \approx 0.15$ . The intensity plots show the fraction of out-coupled atoms as a function of their single-particle energy (normalized to  $E_F$ ) and momentum (normalized to  $k_F$ ), where  $E = 0$  corresponds to a non-interacting particle at rest. The spectra are normalized so that integrating them over momentum and energy gives unity. White dots indicate the centers extracted from gaussian fits to individual energy distribution curves (traces through the data at fixed momentum). The black curve is the quadratic dispersion expected for a free particle. **a** At  $T = 0.74 T_c$ , we observe a BCS-like dispersion with back-bending, consistent with previous measurements [6]. The white curve is a fit to a BCS-like dispersion, Eqn. 1. **b,c** At  $T = 1.24 T_c$  and  $T = 1.47 T_c$ , respectively, the dispersion with back-bending persists even though there is no longer any superfluidity. **d** At  $T = 2.06 T_c$ , the dispersion does not display back-bending in the range of  $0 < k < 1.5 k_F$ . In all the plots there is a negative dispersion for  $k/k_F > 1.5$ . We attribute this weak feature (note the log scale) to a  $1/k^4$  tail and not to the gap.

of pair condensation to determine  $T_c$ , and, momentum-resolved rf spectroscopy to probe the pairing gap, we can now explore the issue of the pseudogap in atomic systems. In this paper, we report that a BCS-like dispersion, with back-bending near  $k_F$ , indeed persists even for temperatures substantially above the measured critical temperature for superfluidity. For the atomic gas system, which is clean and simple in comparison to high  $T_c$  materials, this result demonstrates the existence of a pseudogap region where incoherent pairs of correlated fermions exist above  $T_c$ .

To perform these experiments, we cool a gas of fermionic  $^{40}\text{K}$  atoms to quantum degeneracy in a far detuned optical dipole trap as described in previous work [6]. We obtain a 50/50 mixture of atoms in two spin states, namely the  $|f, m_f\rangle = |9/2, -9/2\rangle$  and  $|9/2, -7/2\rangle$  states, where  $f$  is the total atomic spin and  $m_f$  is the projection along the magnetic-field axis. Our final stage of evaporation occurs at a magnetic field of 203.5 G, where the  $s$ -wave scattering length that characterizes the interactions between atoms in the  $|9/2, -9/2\rangle$  and  $|9/2, -7/2\rangle$  states is approximately  $800 a_0$ , where  $a_0$  is the Bohr radius. At the end of the evaporation we increase the interactions adiabatically with a slow magnetic-field ramp to a Feshbach scattering resonance.

To vary the temperature of the atom cloud, we either truncate the evaporation or parametrically heat the cloud by modulating the optical dipole trap strength at twice the trapping frequency. To determine the temper-

ature of the Fermi gas we expand the weakly interacting gas and fit the momentum distribution to the expected 2D distribution [1] and extract  $(T/T_F)_0$ , where the subscript  $(0)$  indicates a measurement made in the weakly interacting regime, before ramping the magnetic field to the Feshbach resonance. For the data presented here, we obtain clouds at final temperatures ranging from  $(T/T_F)_0 = 0.12$  to  $0.43$  with  $N = 1 \times 10^5$  to  $1.8 \times 10^5$  atoms per spin state. The trap frequencies vary depending on the final intensity of the optical trap and range from 180 to 320 Hz in the radial direction and 18 to 27 Hz in the axial direction. Correspondingly, the Fermi energy,  $E_F$ , ranges from  $h \cdot 8$  kHz to  $h \cdot 13$  kHz, where  $h$  is Planck's constant. The Fermi energy is obtained from  $N$  and the geometric mean trap frequency,  $\nu$ , as  $E_F = \hbar \nu (6N)^{1/3}$ . We define the Fermi wave vector as  $k_F = \frac{\sqrt{2mE_F}}{\hbar}$  and the Fermi temperature as  $T_F = E_F/k_B$ , where  $k_B$  is the Boltzmann constant. It is important to note that the trapped gas has a spatially inhomogeneous density, and one can define a local Fermi energy, and corresponding local Fermi wave vector, that vary across the cloud.

Momentum-resolved rf spectroscopy realizes photoemission spectroscopy for strongly interacting atoms [6], much like angle-resolved photoemission spectroscopy (ARPES) for strongly correlated electron systems. In this spectroscopy, an rf photon flips the spin of an atom to a third hyperfine spin state and then the spin-flipped atoms are counted as function of their momentum. As in ARPES [7], conservation of energy and momentum are

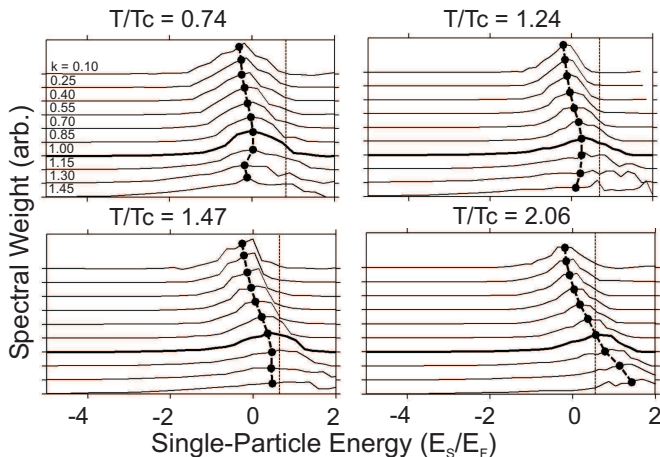


FIG. 2: **Energy Distribution Curves (EDCs)** EDCs are obtained by taking vertical traces at fixed  $k$  through the photoemission spectra shown in Fig. 1. We show EDCs between  $\frac{k}{k_F} = 0.1$  (top) and  $\frac{k}{k_F} = 1.4$  (bottom) for the four data sets with  $T/T_c$  labeled above each figure. Each plotted EDC is an average of EDCs over a range of approximately  $0.15k_F$ . The EDC at  $\frac{k}{k_F} = 1.0$  is shown in bold. Black dots indicate the centers of the gaussian fits to the EDCs. Each EDC is normalized to have an area of unity. Vertical dotted lines are placed at the local  $E_F$  that corresponds to the estimated average density of the gas.

used to extract the energy and momentum of the fermion (which in our case is an entire atom) in the strongly correlated system. A key feature of this measurement is that the spin-flipped atoms are “ejected” from the system in the sense that they have only very weak interactions with the other atoms. This means that the spin-flipped atoms have the usual free-particle dispersion, and moreover, their momentum distribution can be measured using time-of-flight absorption imaging with no significant effects of interactions or collisions on the ballistic expansion. This technique was recently applied to a gas just below  $T_c$  and revealed a BCS-like back-bending dispersion characteristic of an excitation gap [6].

To perform the photoemission experiments on atoms, we turn on a short rf pulse to transfer atoms from the  $|9/2, -7/2\rangle$  state to the unoccupied and weakly-interacting  $|9/2, -5/2\rangle$  state. We then immediately turn off the trap and state-selectively image the out-coupled atoms on a CCD camera after time-of-flight expansion. The rf pulse is kept much shorter than a trap period to ensure that the momentum of the out-coupled atoms does not change. The length of the rf pulse limits our energy resolution to approximately  $0.2E_F$ . As described in our previous work, the intensity of atoms out-coupled as a function of momentum for each rf frequency can be used to reconstruct the occupied single-particle states [6]. With this information, one can determine the occupied part of the Fermi spectral function and probe the energy dispersion. It is important to note that unlike ARPES

experiments in condensed matter physics the value of the chemical potential is not determined in this experiment. Rather, in our plots zero energy corresponds to the energy of a non-interacting atom at rest.

We present our photoemission spectroscopy data studying the pseudogap of a strongly interacting Fermi gas in figures 1 and 2. The dimensionless parameter that characterizes the interaction strength for this data is  $1/k_F a = 0.15(3)$ , where  $a$  is the  $s$ -wave scattering length. In Fig. 1, we plot the fraction of out-coupled atoms as a function of their single-particle energy and momentum for temperatures encompassing the pseudogap regime. In the intensity plots, white dots indicate the centers derived from unweighted gaussian fits to each of the energy distribution curves, or EDCs, (vertical trace at a given wave vector). The energy dispersion mapped out with these fits (white dots) can be contrasted to the expected free particle dispersion for an ideal Fermi gas (black curve). In Fig. 2 we show the same data plotted as EDCs for wavevectors ranging from  $k/k_F = 0.1$  to  $k/k_F = 1.4$ . In order to show the evolution of the spectral function from below  $T_c$  through the pseudogap regime the data are shown for four temperatures,  $(T/T_F)_0 = 0.13, 0.21, 0.25$  and  $0.35$ .

For the data below  $T_c$  (Fig. 1a), we see a smooth back-bending that occurs near  $k = k_F$ . The white curve in Fig. 1a shows a BCS-like dispersion curve, Eqn. 1, discussed above; here, we fit to the white dots for momenta in the range  $0 < k < 1.4k_F$ . While we cannot use this fit to extract the gap and chemical potential in a model-independent way due to the harmonic trapping confinement, the BCS-like fit is consistent with a large pairing gap, on order of  $E_F$ , as expected for a Fermi gas near the center of the BCS-BEC crossover [1, 2].

A striking feature of the data is that the measured spectral function evolves smoothly as the temperature is increased above  $T_c$ . In fact, in all four of our data sets in Fig. 1, we observe a weak signal with a strong negative dispersion at high momenta. It has been recently pointed out that one expects universal behavior at  $k \gg k_F$  for a Fermi gas with short-range, or contact, interactions [23], and, moreover, that this will give rise to a weak, negatively dispersing feature in the Fermi spectral function [24]. Recently, we have directly verified this universal behavior with measurements of the momentum distribution and found empirically that the expected  $1/k^4$  tail occurs for  $k > 1.5k_F$  [25]. Therefore, we attribute the negative dispersion seen at large  $k$  to this universal behavior for contact interactions. While the strength of this feature should reflect the state of the system, the negative dispersion for  $k > 1.5k_F$  does not, by itself, provide evidence of a BCS-pairing gap [24].

In the case of a pairing gap, we expect the spectral function to exhibit back-bending for  $k$  near  $k_F$ . To avoid effects of the universal behavior at large  $k$ , we consider the spectral function for  $k < 1.5k_F$ . For the three low-

est temperatures, we observe a BCS-like dispersion with back-bending behavior that occurs near  $k/k_F = 1$ . We interpret this as evidence for the existence of a pseudogap regime above  $T_c$  comprised of uncondensed pairs in the strongly interacting Fermi gas. At our highest temperature,  $(T/T_F)_0 = 0.35$ , we observe a dispersion that increases quadratically through the region of  $k/k_F = 1$  and then appears to jump discontinuously near  $k/k_F = 1.5$ . At the same point, the amplitudes of the Gaussian fits to the EDCs also drop sharply (see inset to Fig. 3). Thus, we conclude that, as the occupation of the positively dispersing feature vanishes, the fits jump to a distinct, lower energy feature in the spectral function. As discussed above, this lower energy feature is consistent with the predicted effect of universal behavior at large  $k$  on the spectral function [24].

In general, for data taken at finite temperature but still in the pseudogap regime one might expect to see population in the excited branch of the BCS Bogoliubov dispersion (plus sign in Eqn. 1). Signal in this branch represents thermally populated excitations above the pairing gap. The data in the region of  $1 < \frac{k}{k_F} < 1.5$  are suggestive of some occupation in this branch. However, the limited signal-to-noise ratio makes it difficult to identify the excited branch in our data. In addition, the inhomogeneous density of the trapped gas could make the observation of two distinct branches more difficult. To be conservative, we fit each of the EDCs to a single gaussian, and we find this to be sufficient to identify back-bending. It will be a subject of further research to see if the excited branch can be more clearly observed in a momentum-resolved atom photoemission measurement.

In Fig. 3, we directly contrast the dispersions obtained for temperatures  $T/T_c = 0.74, 1.47, \text{ and } 2.06$ , shown in black, red, and green, respectively. We compare the experimental dispersions (circles) to a BCS-BEC crossover theory described in Ref. [4]. To compare to the experimental data, we fit theoretical EDCs to single gaussians to extract the centers; the results are shown as lines in Fig. 3. The theory incorporates the trapping confinement as well as the energy resolution due to the finite rf pulse duration. The theory, which gives the expected  $k^{-4}$  behavior at high  $k$  for the momentum distribution, agrees qualitatively with the experimental data. Both experimental and theoretical dispersions show smooth BCS-like dispersions with back-bending near  $k = k_F$  for temperatures up to  $T/T_c = 1.47$ . For  $T/T_c = 2.06$ , both the experimental and theory show a quadratic dispersion before the signal decays around  $k = 1.5k_F$ , leaving a much weaker negatively dispersing feature as predicted for a normal gas with contact interactions. The apparent disagreement between theory and experiment at  $T/T_c = 0.74$  can be attributed to a sharp variation of the order parameter with temperature close to  $T_c$ . In the inset of Fig. 3, we show the amplitudes of the gaussian fits to the measured EDCs for each of the three temper-

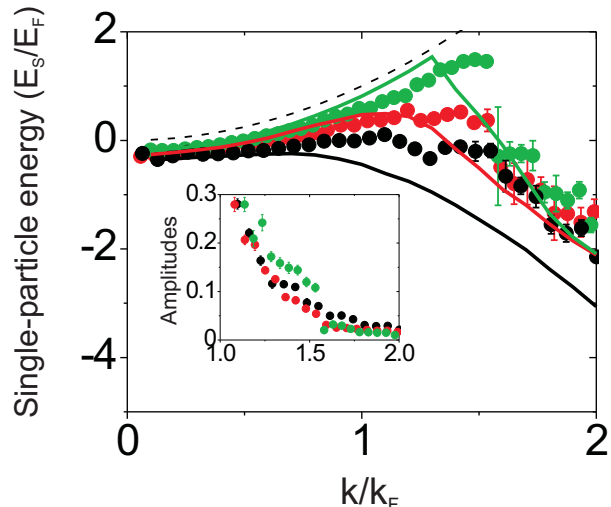


FIG. 3: **Single-particle dispersion curves.** The fits to the EDC centers are shown for the three temperatures in Fig. 1 and Fig. 2 a,c and d, represented by black, red, and green, respectively. We observe a BCS-like dispersion, smooth back-bending near  $\frac{k}{k_F} = 1$ , for temperatures below and moderately above  $T_c$ . For the highest temperature, we observe a quadratic dispersion near  $\frac{k}{k_F} = 1$  and a sharp discontinuity near  $\frac{k}{k_F} = 1.5$ . The lines are theory curves that include effects of the harmonic trap and contact interaction, as described in the text. **Inset** We show the amplitudes from the gaussian fits to the EDCs for the same experimental data. The fit amplitudes evolve smoothly for the lower temperatures but jump discontinuously for the highest temperature gas.

atures.

With theoretical calculations for a homogeneous Fermi gas, we find that the strongly interacting gas with preformed pairs and a normal Fermi liquid have distinct spectral functions. Namely, the paired state shows a smooth avoided crossing (such as described by Eqn. 1) while the normal Fermi liquid exhibits a sharp crossing leading to a cusp or apparent discontinuity in the occupied part of the spectral function. The smooth behavior in the measured dispersion at the three lower temperatures, and the sharp jump in the dispersion at large  $k$  for the highest temperature data are consistent with this theoretical picture.

To determine  $T_c$ , we probe pair condensation in our atomic Fermi gas following the procedure introduced in Ref. [22]. This technique directly probes coherence and has been used to map out  $T_c$  as a function of temperature and interaction strength [22]. The fact that the Bose condensation of fermion pairs corresponds to a superfluid phase transition was demonstrated unambiguously with the observation of a vortex lattice in a rotated Fermi gas below  $T_c$  [26]. In addition, the accuracy of the condensate fraction measurements has been investigated both theoretically [27, 28] and experimentally [29]. In Fig. 4,



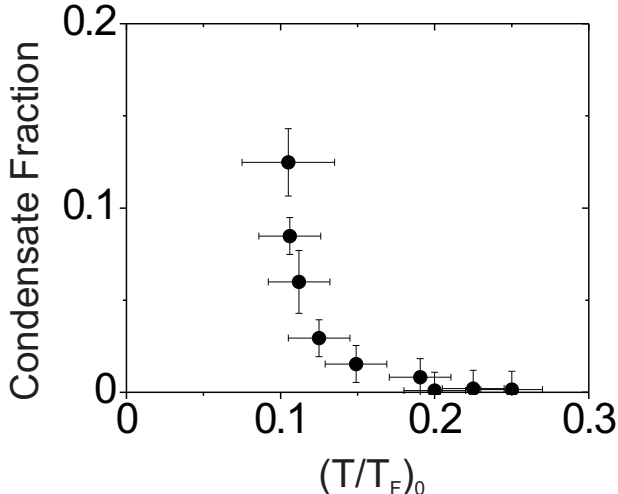


FIG. 4: **Condensate fraction as a function of temperature.** Using time-of-flight expansion at  $B = 202.1$  G where our photoemission experiments are performed, we map out the condensate fraction. Temperature is measured in the weakly interacting regime before the adiabatic ramp to strong interactions. We find  $(\frac{T}{T_F})_0 = 0.17 \pm 0.02$ . Note that the density of the trapped cloud decreases with increasing distance from the trap center, and therefore, in a local density picture, even at  $\frac{T}{T_F} = 0.17$  only the part of the gas at the very center of the trap is below  $T_c$ .

we show the measured pair condensate fraction as a function of the initial temperature of the Fermi gas. As an empirical definition of  $T_c$ , we use the temperature where the measured condensate fraction is 1 %. The value of 1 % is chosen because, when testing our fits with simulated data, we find that we cannot differentiate between a Bose distribution above  $T_c$  and one with a 1 % condensate fraction. We find  $T_c = (0.17 \pm 0.02) T_F$  at  $1/k_F a = 0.15(3)$ , and using this we report  $T/T_c$  for our photoemission spectroscopy data.

Contrasting the photoemission spectroscopy data with this direct measure of the temperature  $T_c$  below which the system has coherent pairs, we find that BCS-like back-bending persists well above  $T_c$  in what we identify to be the pseudogap phase. Above the superfluid transition temperature, these strongly interacting Fermi gases are clearly not described by a Fermi liquid dispersion and the existence of many-body pairing well above  $T_c$  marks a significant departure from conventional BCS theory. It is intriguing to note that our measurements are qualitatively similar to ARPES results in high Tc superconductors [8], even though the atomic Fermi gas is a much simpler system that does not even have an underlying lattice structure. However, high Tc materials and ultracold atom systems differ substantially and for example it may be important to consider that the atomic Fermi gas superfluids have a higher  $\frac{T}{T_F}$  compared to high

Tc superconductors and are more clearly in the region of the BCS-BEC crossover.

## METHODS

### Feshbach resonance location

To create a strongly interacting gas we ramp the magnetic field after evaporation to a value of 202.1 G at a inverse ramp rate of 14 ms/G. The data presented here is at the same magnetic field as previous “on resonance” results presented in Fig. 3b of Ref. [6], where the value of  $a$  was based on a measurement of the resonance position in Ref. [22]. However, from a new measurement based on molecule binding energies determined from rf spectra, we find the resonance position to be  $B_0 = 202.20(2)$  G and width to be  $w = 7.1(2)$  G. With the new resonance parameters and  $B = 202.1$  G, we find that the characteristic dimensionless interaction parameter  $1/k_F a$  is  $0.15(3)$ . This corresponds to the region of the BCS-BEC crossover where the gas is extremely strongly interacting and the superfluid gap is expected to be on order of  $E_F$ . Note that in the absence of many-body physics, the two-body prediction of the molecule binding energy at 202.1 G is 480 Hz, which is less than  $0.05E_F$ .

### Photoemission spectroscopy

For the work presented here, we have improved the signal-to-noise ratio of the photoemission spectra by a factor of four compared to our previous measurement [6]. Previously, a limitation to the signal-to-noise was related to imaging the out-coupled  $|9/2, -5/2\rangle$  atoms, which lack a closed cycling transition for absorption imaging. Now, we transfer the out-coupled atoms to the  $|9/2, -9/2\rangle$  state with two rf  $\pi$ -pulses. Because the number of atoms in the  $|9/2, -5/2\rangle$  state is relatively small, this requires that we first optically pump the atoms remaining in the  $|9/2, -7/2\rangle$  and  $|9/2, -9/2\rangle$  states to another hyperfine manifold. In this way, we can image the out-coupled atoms with the cycling transition for the  $|9/2, -9/2\rangle$  state without contamination from the much larger population of atoms that were unaffected by the rf spectroscopy. Before constructing the photoemission spectra, we clean up the raw images by setting to zero data at large radii where the signal drops below technical noise.

### Density inhomogeneity of the trapped gas

One can define a local Fermi energy, and corresponding local Fermi wave vector, that vary across the cloud. We can estimate average density of the strongly interacting gas by taking the average density of an ideal trapped Fermi gas at a particular  $\frac{T}{T_F}$  and multiplying by  $(\frac{E_{pot}}{E_{pot}^0})^{-3/2}$ . Here,  $\frac{E_{pot}}{E_{pot}^0}$  is the measured ratio (at finite  $T$ ) of the potential energy of the strongly interacting gas to that of a non-interacting gas [30]. For the the data shown in Fig. 1 a-d, the local Fermi energy, in units of the previously defined  $E_F$ , that corresponds to this aver-

age density is 0.81, 0.69, 0.62, and 0.53, respectively. The corresponding local Fermi wave vector, in units of  $k_F$ , is 0.90, 0.83, 0.79, and 0.73, respectively. To give a sense of the spread in the local Fermi energies, we note that for the ideal trapped Fermi gas, the ratio of the local Fermi energy at the average density to that at the cloud center is approximately 0.6.

We acknowledge funding from the NSF. We thank the JILA BEC group for discussions. DSJ acknowledges discussions with A. Kanigel at the Aspen Center for Physics.

- 
- [1] C. A. Regal and D. S. Jin, *Adv. Atom. Mol. Opt. Phys.* **54**, 1 (2006).
- [2] W. Ketterle and M. W. Zwierlein, in *Proceedings of the International School of Physics "Enrico Fermi", Course CLXIV*, edited by M. Inguscio, W. Ketterle, and C. Salomon (IOS Press, Amsterdam, 2008).
- [3] M. Randeria, in *Proceedings of the International School of Physics "Enrico Fermi", Course CXXXVI*, edited by G. Iadonisi, J. R. Schrieffer, and M. L. Chialfalo (IOS Press, Amsterdam, 1998).
- [4] A. Perali, P. Pieri, G. C. Strinati, and C. Castellani, *Phys. Rev. B* **66**, 024510 (2002).
- [5] Q. Chen, J. Stajic, and K. Levin, *Low Temp. Phys.* **32**, 406 (2006).
- [6] J. T. Stewart, J. P. Gaebler, and D. S. Jin, *Nature* **454**, 744 (2008).
- [7] A. Damascelli, *Physica Scripta* **T109**, 61 (2004).
- [8] A. Kanigel *et al.*, *Phys. Rev. Lett.* **101**, 137002 (2008).
- [9] M. Randeria, N. Trivedi, A. Moreo, and R. T. Scalettar, *Phys. Rev. Lett.* **69**, 2001 (1992).
- [10] C. A. R. Sá de Melo, M. Randeria, and J. R. Engelbrecht, *Phys. Rev. Lett.* **71**, 3202 (1993).
- [11] B. Janko, J. Maly, and K. Levin, *Phys. Rev. B* **56**, R11407 (1997).
- [12] Y. Yanase and K. Yamada, *J. Phys. Soc. Jpn* **68**, 2999 (1999).
- [13] G. M. Bruun and G. Baym, *Phys. Rev. A* **74**, 033623 (2006).
- [14] P. Massignan, G. M. Bruun, and H. T. C. Stoof, *Phys. Rev. A* **77**, 031601(R) (2008).
- [15] N. Barnea, *Phys. Rev. A* **78**, 053629 (2008).
- [16] P. Magierski, G. Wlazlowski, A. Bulgac, and J. E. Drut, *Phys. Rev. Lett.* **103**, 210403 (2009).
- [17] Q. Chen, Y. He, C. C. Chien, and K. Levin, *Rep. Prog. Phys.* **72**, 122501 (2009).
- [18] S. Tsuchiya, R. Watanabe, and Y. Ohashi, *Phys. Rev. A* **80**, 033613 (2009).
- [19] R. Haussmann, M. Punk, and W. Zwerger, *Phys. Rev. A* **80**, 063612 (2009).
- [20] C. Chin *et al.*, *Science* **305**, 1128 (2004).
- [21] A. Schirotzek, Y. Shin, C. H. Schunck, and W. Ketterle, *Phys. Rev. Lett.* **101**, 140403 (2008).
- [22] C. A. Regal, M. Greiner, and D. S. Jin, *Phys. Rev. Lett.* **92**, 040403 (2004).
- [23] S. Tan, *Annals of Physics* **323**, 2971 (2008).
- [24] W. Schneider and M. Randeria, *Phys. Rev. A* **81**, 021601 (2010).
- [25] J. T. Stewart, J. P. Gaebler, T. E. Drake, and D. S. Jin, arXiv:1002.1987 (unpublished).
- [26] M. W. Zwierlein *et al.*, *Nature* **435**, 1047 (2005).
- [27] A. Perali, P. Pieri, and G. C. Strinati, *Phys. Rev. Lett.* **95**, 010407 (2005).
- [28] S. Matyjaśkiewicz, M. H. Szymańska, and K. Góral, *Phys. Rev. Lett.* **101**, 150410 (2008).
- [29] M. W. Zwierlein *et al.*, *Phys. Rev. Lett.* **94**, 180401 (2005).
- [30] J. T. Stewart, J. P. Gaebler, C. A. Regal, and D. S. Jin, *Phys. Rev. Lett.* **97**, 220406 (2006).